# A Computational Study on the Templating Ability of the Trispyrrolidinium Cation in the Synthesis of ZSM-18 Zeolite

Maria J. Sabater and German Sastre*

*Instituto de Tecnologia Quimica UPV-CSIC, Universidad Politecnica de Valencia, Avenida Los Naranjos s/n, 46022 Valencia, Spain*

*Received February 27, 2001. Revised Manuscript Received September 12, 2001*

The role of trispyrrolidinium cation as the structure-directing agent of the ZSM-18 zeolite structure is explained by a close matching between the template and the zeolite walls. Two template orientations are proposed, and their respective structure-directing abilities are discussed in terms of template−zeolite energetic interactions. The relation of the template orientation and the Al distribution of the ZSM-18 structure is explained, and the preferential substitution of Al in the three-membered rings of ZSM-18 is explained from the results of the calculations, in accordance with the XRD solution of the structure.

## 1. Introduction

Many of the novel silica-based zeolite structures are derived from the use of suitable organic additives in the synthesis process as structure-directing agents (SDAs) which allow selection between possible phases of similar thermodynamic stability.[1,2] Three roles have been proposed for these organic species: space-filling agents, structure-directing agents, and templates.[3−6] The former does not appear to offer any control of product pore architectures, and sometimes the material can be synthesized by an organic-free route.[7] In the latter two there is a close correspondence between the structure of the organic molecule and the pore topology, and in some cases (SDAs) the organic molecule directs the synthesis toward a particular zeolite structure. Recently, some new zeolite structures have been synthesized in our group with the help of SDAs.[8−11] The synthesis of new structures is guided by many experimental factors, and considerable advancement has been achieved over the past decade, in particular regarding the role of the SDAs in the synthesis, but many questions remain to be answered, and in fact it is recognized that the outcome of a new synthetic route cannot be predicted a priori. Certainly, breakthroughs in the synthesis of new zeolite structures come nowadays by an adequate design of the experimental conditions of synthesis. This particular field represents a good ground to test new combinatorial chemistry methods adapted to the specific task of finding new microporous materials. But it is no less important to push forward the basic understanding of several aspects of the synthetic process such as the conditions necessary for the existence of a true templating effect. It is then that molecular simulations come into play. The huge number of experimental factors that influence the synthesis cannot be accurately simulated by any technique available today, and drastic approximations have to be made. Nevertheless, despite this apparent shortcoming, interesting results have been obtained by using force field methodologies for instance. Lewis et al.[12] have used a combined Monte Carlo and energy minimization technique to calculate the stability and location of tetraalkylammonium cations in ZSM-5, ZSM-11, and $\beta$ zeolites as well as bisquaternary amines in EU-1 and ZSM-23, and the results allow the selection of the most appropriate templates for the synthesis of those structures. A similar technique is used by Lewis et al.[13] to find the influence of the template molecule and Co concentration in the competitive formation of Co−AlPO-5 and Co−AlPO-34 from the same synthesis gel. Also, Monte Carlo docking algorithms based on a force field approach combined with crystallographic data have been used by Toby et al.[14] to study the effect of structure-directing agents in the inhibition or formation of stacking faults in CIT-1. A number of other studies based on computer simulation of the rationalization of zeolite synthesis are available in the literature,[15−19] and they show an increasing availability of possibilities to justify and predict the stability of organic species occluded in

* To whom correspondence should be addressed.

(1) Davis, M. E.; Lobo, R. F. *Chem. Mater.* **1992**, *4*, 756.
(2) Petrovic, I.; Navrotsky, A.; Davis, M. E.; Zones, S. I. *Chem. Mater.* **1993**, *5*, 1805.
(3) Barrer, R. M. *Zeolites* **1981**, *1*, 130.
(4) Barrer, R. M. *Stud. Surf. Sci. Catal.* **1985**, *24*, 1.
(5) Lok, B. M.; Cannan, T. R.; Messina, C. A. *Zeolites* **1983**, *3*, 282.
(6) Davis, M. E. *Acc. Chem. Res.* **1993**, *26*, 111.
(7) Hong, S. B.; Cho, H. M.; Davis, M. E. *J. Phys. Chem.* **1993**, *97*, 1622.
(8) Barrett, P. A.; Camblor, M. A.; Corma, A.; Jones, R. H.; Villescusa, L. A. *Chem. Mater.* **1997**, *9*, 1713.
(9) Villaescusa, L. A.; Barrett, P. A.; Camblor, M. A. *Chem. Commun.* **1998**, 2329.
(10) Villaescusa, L. A.; Barrett, P. A.; Camblor, M. A. *Angew. Chem., Int. Ed.* **1999**, *38*, 1997.
(11) Corma, A.; Diaz-Cabañas, M. J.; Fornes, V. *Angew. Chem., Int. Ed.* **2000**, *39*, 2346.
(12) Lewis, D. W.; Freeman, C. F.; Catlow, C. R. A. *J. Phys. Chem. B* **1995**, *99*, 11194.
(13) Lewis, D. W.; Catlow, C. R. A.; Thomas, J. M. *Chem. Mater.* **1996**, *8*, 1112.
(14) Toby, B. H.; Khosrovani, N.; Dartt, C. B.; Davis, M. E.; Parise, J. B. *Microporous Mesoporous Mater.* **2000**, *39*, 77.

10.1021/cm0110526 CCC: $20.00 
Published on Web 11/30/2001

microporous materials and their templating ability. In particular, some recent studies by Shantz et al.[20] explain how the distribution of framework aluminum in ZSM-12 can be controlled by the template location.

The synthesis of ZSM-18 (with International Zeolite Association code MEI[21]) in the presence of the trispyrrolidinium cation[22] is a templating effect caused by the close conformation between the organic molecule and the zeolite micropore.[23,24] In the presence of this cation, the ZSM-18 is formed specifically within a broad range of synthetic conditions which do not give the structure in the absence of the template.[25] Previous studies of the structure-directing effect have focused on the correlation with van der Waals match between the organic and the zeolite cavity, and in this case we analyze the different energetic terms of interaction between the template and the zeolite. The aim of the present study is to apply atomistic computational methods to study the specifity between the trispyrrolidinium cation and the ZSM-18 and also investigate whether the Al location in the ZSM-18 zeolite occurs randomly or there is some influence of the energetics of the Al structural incorporation and the host−guest interactions between the template and the zeolite structure.

## 2. Methodology

The calculations were performed using lattice energy minimization techniques and the GULP code.[26] The interatomic potentials used to model the interactions between the atoms in the structure included the following terms: Coulombic interaction, short-range pair potentials (described by a Buckingham function), and a three-body bond bending term. The shell model was used to simulate the polarizability of the oxygen atoms. A cutoff distance of 12 Å was applied to the short-range interactions (Buckingham- and Lennard-Jones-type interactions; see eqs 3 and 12 below). The Ewald summation technique was used for the summation of the long-range Coulombic interactions. The potentials used for the zeolite[27−29] were parametrized to reproduce the structure of the α-quartz and $Al_2O_3$ and have further been demonstrated to successfully model a number of zeotype structures.[30,31] The Si−O and Al−O potential parameters have been extensively used in modeling the structures of zeolites.[32,33] The total potential energy function and the respective terms are as follows:

$$V_{\text{total}} = V_{\text{zeo}} + V_{\text{template}} + V_{\text{template-template}} + V_{\text{zeo-template}} \quad (1)$$

$$V_{\text{zeo}} = V_{\text{Buckingham}} + V_{\text{Coulombic}} + V_{\text{three-body}} + V_{\text{core-shell}} \quad (2)$$

$$V_{ij}(\text{Buckingham}) = A_{ij} \exp(-r_{ij}/\rho) - C_{ij}/r^6 \quad (3)$$

$$V_{ij}(\text{Coulombic}) = (q_i q_j)/r_{ij} \quad (4)$$

$$V_{ijk}(\text{three-body}) = {}^1/_2 k_{ijk}(\theta_{ijk} - \theta_{ijk}{}^0)^2 \quad \text{with} \quad \theta = \text{O-T-O} \quad (5)$$

$$V_{ij}(\text{core-shell}) = {}^1/_2 k_{ij}(r_{ij} - r_{ij}{}^0)^2 \quad (6)$$

$$V_{\text{template}} = V_{\text{two-body}} + V_{\text{three-body}} + V_{\text{four-body}} + V_{\text{Coulombic}} \quad (7)$$

$$V_{ij}(\text{two-body}) = {}^1/_2 k_{ij}(r_{ij} - r_{ij}{}^0)^2 \quad (8)$$

$$V_{ijkl}(\text{four-body}) = A_{ijkl}[1 + \cos(n\phi_{ijkl} - \delta_{ijkl})] \quad (9)$$

$$V_{\text{template-template}} = V_{\text{Lennard-Jones}} + V_{\text{Coulombic}} \quad (10)$$

$$V_{\text{zeo-template}} = V_{\text{Lennard-Jones}} + V_{\text{Coulombic}} \quad (11)$$

$$V_{ij}(\text{Lennard-Jones}) = B_{ij}/r^{12} - C_{ij}/r^6 \quad (12)$$

We employed the Mott−Littleton methodology to treat the incorporation of defects within the perfect lattice. This widely used method allows the full relaxation of atomic coordinates of an inner region (100−500 ions), surrounding the defect, to minimum energy, while more distant regions of the crystal are treated as a dielectric continuum. The force field by Kiselev et al.[34] was selected for the intermolecular template−zeolite and template−template interactions, and the force field by Oie et al.[35] was selected for intramolecular interactions between the atoms of the template. The force field parameters are listed in Table 1. The template used in the synthesis of ZSM-18[23] is the triply charged cation 2,3,4,5,6,7,8,9-octahydro-2,2,5,5,8,8-hexamethyl-1*H*-benzo[1,2-*c*:3,4-*c*:5,6-*c*]tripyrrolium (trispyrrolidinium cation). To treat in a realistic way the electrostatics of the interaction between the template and the zeolite, a previous full optimization of the triply charged template was obtained by the ab initio Hartree−Fock methodology with the 6-31G** basis set by using the NWChem[36] package. The corresponding charges are listed in Table 1.

## 3. Results and Discussion

**3.1. Structural Aspects of ZSM-18.** ZSM-18 has been described previously,[23] and it is a zeolite with a

(15) (a) Catlow, C. R. A.; Coombes, D. S.; Lewis, D. W.; Pereira, J. C. G. *Chem. Mater.* **1998**, *10*, 3249. (b) Lewis, D. W.; Willock, D. J.; Catlow, C. R. A.; Thomas, J. M.; Hutchings, G. J. *Nature* **1996**, *382*, 604. (c) Lewis, D. W.; Sankar, G.; Wyles, J. K.; Thomas, J. M.; Catlow, C. R. A.; Willock, D. J. *Angew. Chem., Int. Ed. Engl.* **1997**, *36*, 2675.
(16) Bull, I.; Villaescusa, L. A.; Teat, S. J.; Camblor, M. A.; Wright P. A.; Lightfoot, P.; Morris, R. E. *J. Am. Chem. Soc.* **2000**, *122*, 7128.
(17) Camblor, M. A.; Villaescusa, L. A.; Diaz-Cabañas, M. J. *Top. Catal.* **1999**, *9*, 59.
(18) van de Graaf, B.; Njo, S. L.; Smirnov, K. S. *Rev. Comput. Chem.* **2000**, *14*, 137.
(19) Wagner, P.; Nakagawa., Y.; Lee, G. S.; Davis, M. E.; Elomari, S.; Medrud, R. C.; Zones, S. I. *J. Am. Chem. Soc.* **2000**, *122*, 263.
(20) (a) Shantz, D. F.; Lobo, R. F.; Fild, C.; Koller, H. *Stud. Surf. Sci. Catal.* **2000**, *130*, 845. (b) Shantz, D. F.; Schmedt auf der Günne, J.; Koller, H.; Lobo, R. F. *J. Am. Chem. Soc.* **2000**, *122*, 6659. (c) Shantz, D. F.; Fild, C.; Koller, H.; Lobo, R. F. *J. Phys. Chem. B* **1999**, *103*, 10858.
(21) Meier, W. M.; Olson, D. H.; Baerlocher, C. *Atlas of Zeolite Structure Types*, 4th ed.; Elsevier: Amsterdam, 1996. Also URL http://www.iza-structure.org.
(22) Lawton, S. L.; Ciric, J.; Kokotailo, G. *Acta Crystallogr., C* **1985**, *41*, 1683.
(23) Lawton, S. L.; Rohrbaugh, W. J. *Science* **1990**, *247*, 1319.
(24) Geisinger, K. L.; Gibbs, G. V.; Navrotsky, A. *Phys. Chem. Miner.* **1985**, *11*, 266.
(25) Schmitt, K. D.; Kennedy, G. J. *Zeolites* **1994**, *14*, 635.
(26) Gale, J. D. *J. Chem. Soc., Faraday Trans.* **1997**, *93*, 629.
(27) Sanders, M. J.; Leslie, M.; Catlow, C. R. A. *J. Chem. Soc., Chem. Commun.* **1984**, 1271.
(28) Jackson, R. A.; Catlow, C. R. A. *Mol. Simul.* **1988**, *1*, 207.
(29) *Computer Simulations of Solids*; Catlow, C. R. A., Mackrodt, W. C., Eds.; Lecture Notes in Physics No. 166; Springer-Verlag: Berlin, 1982.
(30) Henson, N. J.; Cheetham, A. K.; Gale, J. D. *Chem. Mater.* **1994**, *6*, 1647.
(31) Henson, N. H.; Cheetham, A. K.; Gale, J. D. *Chem. Mater.* **1996**, *8*, 664.
(32) *Modelling of Structure and Reactivity in Zeolites*; Catlow, C. R. A., ed.; Academic Press: London, 1992.
(33) Catlow, C. R. A.; Bell, R. G.; Gale, J. D. *J. Mater. Chem.* **1994**, *4*, 781.
(34) Kiselev, A. V.; Lopatkin, A. A.; Shulga, A. A. *Zeolites* **1985**, *5*, 261.
(35) Oie, T.; Maggiora, T. M.; Christoffersen, R. E.; Duchamp, D. J. *Int. J. Quantum Chem., Quantum Biol. Symp.* **1981**, *8*, 1.
(36) Harrison, R.; Nichols, J.; Straatsma, T.; Dupuis, M.; Bylaska, E.; Fann, G.; Windus, T.; Apra, E.; Anchell, J.; Bernholdt, D.; Borowski, P.; Clark, T.; Clerc, D.; Dachsel, H.; de Jong, B.; Deegan, M.; Dyall, K.; Elwood, D.; Fruchtl, H.; Glendenning, E.; Gutowski, M.; Hess, A.; Jaffe, J.; Johnson, B.; Ju, J.; Kendall, R.; Kobayash, R.; Kutteh, R.; Lin, Z.; Littlefield, R.; Long, X.; Meng, B.; Nieplocha, J.; Niu, S.; Rosing, M.; Sandrone, G.; Stave, M.; Taylor, H.; Thomas, G.; van Lenthe, J.; Wolinski, K.; Wong, A.; Zhang, Z. *NWChem, A Computational Chemistry Package for Parallel Computers*, version 4.0; Pacific Northwest National Laboratory: Richland, WA, 2000.

**Table 1. Potential parameters used within the GULP Code[a]**

| Atomic Charges | | | | | |
|---|---|---|---|---|---|
| Si | core | 4.00000 | C2 | core | −0.01130 |
| Al | core | 3.00000 | C1 | core | −0.07150 |
| O | core | 0.86902 | N4 | core | −0.16540 |
| O | shell | −2.86902 | H2 | core | 0.13220 |
| C6 | core | 0.01380 | H1 | core | 0.12910 |

Buckingham (Intramolecular for Zeolite, Eq 3, Refs 27 and 28)

| *i* | *j* | $A_{ij}$ (eV) | $\rho_{ij}$ (Å$^{-1}$) | $C_{ij}$ (eV·Å$^6$) |
|---|---|---|---|---|
| Al | O | 1460.300 | 0.29912 | 0.000 |
| O | O | 22764.000 | 0.14900 | 27.880 |
| Si | O | 1283.907 | 0.32052 | 10.662 |

Three-Body (Intramolecular for Zeolite, Eq 5, Refs 27 and 28)

| *i* | *j* | *k* | $k_{ijk}$ (eV/rad$^2$) | $\theta_{ijk}^0$ (deg) |
|---|---|---|---|---|
| O | Al | O | 2.0972 | 109.47 |
| O | Si | O | 2.0972 | 109.47 |

Spring (Intraatomic for Oxygens in Zeolite, Eq 6, Ref 27)

| *i* | *j* | $k_{ij}$ (eV/Å$^2$) |
|---|---|---|
| $O_{core}$ | $O_{shell}$ | 74.92 |

Harmonic (Intramolecular for Template, Eq 8, Ref 35)

| *i* | *j* | $k_{ij}$ (eV/Å$^2$) | $r_{ij}^0$ (Å) |
|---|---|---|---|
| C6 | C6 | 48.94 | 1.385 |
| C6 | C2 | 31.75 | 1.510 |
| C2 | N4 | 28.75 | 1.495 |
| C1 | N4 | 28.75 | 1.495 |
| C2 | H | 28.71 | 1.095 |
| C1 | H | 28.71 | 1.095 |

Three-Body (Intramolecular for Template, Eq 5, Ref 35)

| *i* | *j* | *k* | $k_{ijk}$ (eV/Å$^2$) | $\theta_{ijk}^0$ (deg) |
|---|---|---|---|---|
| C6 | C6 | C6 | 3.44 | 120.0 |
| N4 | C1 | H | 2.50 | 109.5 |
| N4 | C2 | H | 2.50 | 109.5 |
| C6 | C6 | C2 | 3.44 | 120.0 |
| C6 | C2 | H | 2.50 | 109.0 |
| C2 | N4 | C1 | 6.87 | 109.0 |
| C2 | N4 | C2 | 6.87 | 109.0 |
| C1 | N4 | C1 | 6.87 | 109.0 |
| H | C2 | H | 2.06 | 109.1 |
| H | C1 | H | 2.06 | 109.2 |
| N4 | C2 | C6 | 3.56 | 111.0 |

Torsion (Intramolecular for Template, Eq 9, Ref 35)

| *i* | *j* | *k* | *l* | $A_{ijkl}$ (eV) | n | $\delta_{ijkl}$ (deg) |
|---|---|---|---|---|---|---|
| C6 | C6 | C2 | N4 | 0.0035 | 3 | 0.0 |
| C6 | C2 | N4 | C2 | 0.0035 | 30.0 | |
| C6 | C2 | N4 | C1 | 0.0035 | 3 | 0.0 |
| C6 | C6 | C6 | C6 | 0.2166 | 2 | 180.0 |
| C6 | C6 | C6 | C2 | 0.0867 | 2 | 180.0 |
| C6 | C6 | C2 | H | 0.0043 | 3 | 0.0 |
| C2 | N4 | C2 | H | 0.0175 | 3 | 0.0 |
| C2 | N4 | C1 | H | 0.0175 | 3 | 0.0 |
| C2 | C6 | C6 | C2 | 0.2166 | 2 | 180.0 |
| C1 | N4 | C2 | H | 0.0175 | 3 | 0.0 |
| C1 | N4 | C1 | H | 0.0175 | 3 | 0.0 |

Lennard-Jones (Intermolecular for Template−Template, Eq 12, Ref 34)

| *i* | *j* | $B_{ij}$ (eV·Å$^{12}$) | $C_{ij}$ (eV·Å$^6$) |
|---|---|---|---|
| C | C | 19692.00 | 18.0933 |
| C | H | 2800.00 | 5.8415 |
| H | H | 384.84 | 1.9867 |
| N | H | 1803.37 | 6.0653 |

Lennard-Jones (Intermolecular for Template−Zeolite, Eq 12, Ref 34)

| *i* | *j* | $B_{ij}$ (eV·Å$^{12}$) | $C_{ij}$ (eV·Å$^6$) |
|---|---|---|---|
| H | O | 1556.40 | 5.5717 |
| C | O | 11000.00 | 17.6540 |
| N | O | 7761.38 | 18.5467 |

[a] The atoms of the trispyrrolidinium cation are as follows: N4 is quaternary nitrogen, C6 is carbon in the benzene ring, C1 and C2 are primary and secondary carbons, respectively, and H1 and H2 are hydrogens bonded to C1 and C2, respectively.

**Table 2. Geometric Analysis of the MEI Structure[23]**

| T−O label | distance (Å) | T−O label | distance (Å) | T−O label | distance (Å) |
|---|---|---|---|---|---|
| T1−O6 | 1.62 | T3−O7 | 1.61 | T3−O11 | 1.61 |
| T2−O6 | 1.61 | T2−O8 | 1.62 | T3−O9 | 1.61 |
| T1−O5 | 1.58 | T3−O8 | 1.62 | T4−O9 | 1.60 |
| T2−O7 | 1.61 | T2−O11 | 1.61 | T4−O10 | 1.63 |

| T−O−T label | angle (deg) | T−O−T label | angle (deg) | T−O−T label | angle (deg) |
|---|---|---|---|---|---|
| T1−O6−T2 | 147.4 | T2−O8−T3 | 142.5 | T4−O10−T4 | 134.7 |
| T1−O5−T1 | 180.0 | T2−O11−T3 | 147.7 | | |
| T2−O7−T3 | 150.9 | T3−O9−T4 | 149.6 | | |

channel system of 12-MRs (12-membered rings) intersected with 7-MR openings. The 12-MR channel runs parallel to the [001] direction, whereas the 7-MR openings are perpendicular to the 12-MR channel. It is noted that the 12-MRs and the 7-MRs lie at different heights in the [001] direction, and this implies that the room available for molecules inside the structure is different at the height of the 12-MRs and at the expanded region resulting from the 7-MR apertures in the 12-MR channel.

The structure of ZSM-18 contains four different T (Si, Al) atoms. A particularity of the ZSM-18 is the presence of unusual 3-MRs, which in this case are made of Si4-type T atoms. The average TOT angles (Table 2) corresponding to the reported calcined structure[23] indicate that the smallest angles are those present within the 3-MRs, i.e., Si4−O10−Si4 angles, and this may be related to a certain local strain in that part of the ZSM-18 structure. When Al is incorporated into the framework positions, it is difficult to say a priori whether that strain may be partially released by a preferential substitution of Al atoms in the T4 position. This will depend on the relative ability of the structure to minimize the total energy when the Al atoms are introduced in the different available positions, and henceforth, the local strain (in this case in the 3-MRs) is only a component of that total energy. It is clearly inferred that the computer simulation is of help in assessing the Al stability in the four different T sites, and with this in mind a preliminary set of defect calculations have been carried out. Prior to the analysis of the calculations it should be remarked that the calculations correspond to the calcined structure, and thus the effect of Al stabilization by the effect of the template is not taken into account. This will be considered later.

The defect calculations have been performed over a single unit cell of composition $Si_{34}O_{68}$ to which a defect substitution, Si → Al, was performed in each of the four T positions present in ZSM-18. Defect energies[37] do refer to the process of taking a Si(4+) from the framework to infinity and taking an Al(3+) from infinity to the vacant framework position. These energies do not correspond to the reality of Al substitution, but they serve on a comparative basis to state the relative stability of the possibilities considered. The calculated energies are shown in Table 3, and it is observed that the T4 position is the least preferential for the accommodation of the incoming Al atom in the zeolite framework. This would

(37) Sastre, G.; Lewis, D. W.; Catlow, C. R. A. *J. Phys. Chem.* **1996**, *100*, 6722.

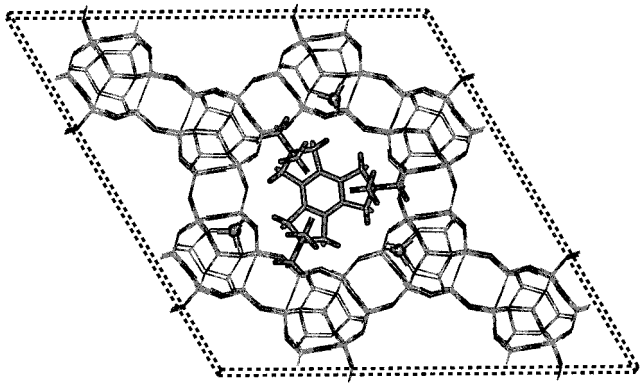

**Figure 1.** ZSM-18 and template located parallel to the plane of the sheet. The Al atoms in the framework are highlighted with spheres. The Al distribution corresponds to the initial configuration.

**Table 3. Defect Energies of the Si → Al Substitution over the Four T Sites in the MEI Structure**

| T label | energy (eV) | rel energy (kJ/mol) | T label | energy (eV) | rel energy (kJ/mol) |
|---|---|---|---|---|---|
| T1 | 37.9230 | 0.0 | T3 | 38.1004 | 17.1 |
| T2 | 38.0635 | 13.6 | T4 | 38.2461 | 31.2 |

point to a preferential Al location in positions T1, T2, T3, and finally T4, which would be the least favored. The same result was previously found by Gale et al.[38] The experimental structural determination gave us a hint of the preferred Al location by examining the T−O distances, which correspond to a ZSM-18 structure[23] synthesized with a Si/Al ratio between 5 and 15, which means that the T−O distances correspond to an average of Si and Al atoms. The largest distance (Table 2) corresponds to the T4−O10 pair (1.63 Å). Taking into account the well-known fact that Al−O distances are larger than Si−O distances,[39] it follows that the preferential Al location is expected in position T4, in clear contradiction with the calculations reported above. This leads us to think that it is not the framework stability that directs the Al location but rather the interaction of Al atoms with the template, an interaction which is in part controlled by electrostatic factors as we will see later. It follows from here the importance of finding the optimized location(s) of the template in the structure of ZSM-18.

**3.2. Optimization of the Template in the Void Space of ZSM-18.** The hexagonal $P6_3/m$ unit cell of ZSM-18[23] with cell parameters $a = 13.18$ Å and $c = 15.85$ Å and stoichiometry $Si_{34}O_{68}$ was used as a starting point, and from this, a $2 \times 2 \times 2$ supercell with three Al atoms ($Si_{269}Al_3O_{544}$) was generated for the calculations. The tricationic template was initially inserted into the void space of ZSM-18 in two different configurations that we call "parallel" (Figure 1) and "perpendicular" (Figure 2) to the 12-MR channel in the [001] direction.

Two slightly different conformations of the template, with symmetries $C_{3v}$ and $C_s$, have been found in the gas phase by applying first principles and force field calculations.[40] The two conformations differ in the puckering

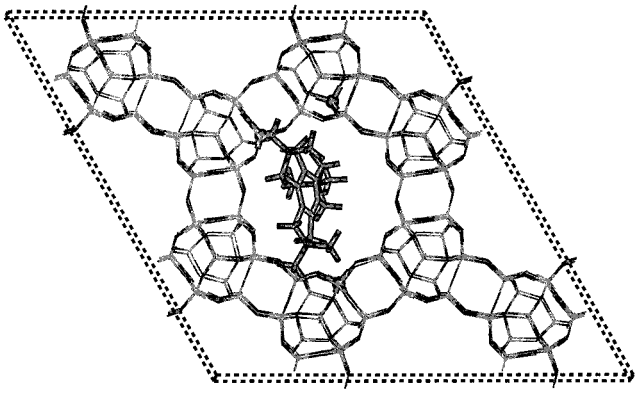

**Figure 2.** ZSM-18 and template located perpendicular to the plane of the sheet. The Al atoms in the framework are highlighted with spheres. The Al distribution corresponds to the initial configuration.

of the pyrrolium rings with respect to the benzene plane. In the $C_{3v}$ symmetry the three pyrrolium rings are puckered toward the same side of the benzene ring, whereas in the $C_s$ symmetry two pyrrolium rings are puckered to one side and one pyrrolium ring is puckered to the opposite side of the benzene plane. The experimental puckering angle is 30.6°, and the energy difference between the two conformations is within 1 kcal/mol, the $C_s$ conformation being the most stable. In our energy minimizations of the tricationic template inside the ZSM-18 structure, all the coordinates of the template will be allowed to relax; therefore, none of the gas-phase conformations will be imposed, but rather the interactions of the template with the zeolite will define which conformation is preferred.

Initially, the minimizations were carried out by initially fixing the coordinates of the zeolite framework and keeping the cell parameters to the crystallographically reported. This is what we call "partial optimization". This was done, not for the sake of saving computational time (a total of 1411 core + shell units is not a serious penalty for a full optimization with our computational resources), but rather for the sake of having the same microporous framework in the two optimizations and henceforth allowing a direct comparison between the two template orientations analyzed in this study. In this way, both the internal coordinates of the template plus its orientation with respect to the ZSM-18 cavity were allowed to move during this energy minimization. The triply positive charge of the template is compensated by the presence of three Al atoms replacing the Si atoms in the zeolite framework, thus preserving the electroneutrality of the system. Initially, the three Al atoms in the zeolite framework were not placed randomly but in the closest positions to the respective three nitrogen atoms of the template. We believe this is a reasonable starting point as the negative charge brought by Al in the zeolite framework may tend to be near the positive charge concentration within the template, i.e., along the methyl groups bonded to the nitrogen atoms. In a subsequent section other possibilities for the Al distribution will be explored. The final energies after the partial minimization are shown in Table 4, and the difference between them is 0.34 eV (32.8 kJ/mol). The most stable configuration corresponds to the parallel orientation, and this is the one proposed after the XRD structure determination,

(38) Gale, J. D.; Cheetham, A. K. *Zeolites* **1992**, *12*, 674.
(39) Gibbs, G. V. *Am. Mineral.* **1982**, *67*, 421.
(40) Koelmel, C. M.; Li, Y. S.; Freeman, C. M.; Levine, S. M.; Hwang, M.-J.; Maple, J. R.; Newsam, J. M. *J. Phys. Chem.* **1994**, *98*, 12911.

**Table 4. Energy (eV) of the Total System Zeolite + Template after Minimization[a]**

| optimization | parallel | perpendicular |
|---|---|---|
| partial | −34475.5515 | −34475.2067 |
| full | −34836.9024 | −34836.8299 |

[a] Two template orientations have been considered as discussed in the text (parallel and perpendicular as in Figures 1 and 2, respectively).

so our calculations suggest the same template orientation within the zeolite void space. It is also interesting to remark that the perpendicular template orientation may be a reasonable alternative which could also be proposed. Before further exploring this possibility, we carried out a "full optimization" to confirm or rule out the validity of the previous results. In this case, all the atoms of the system and also the cell parameters were allowed to relax. The total CPU time employed by our SGI Origin2000 (with CPU R10k IP27 at 180 MHz) for the full optimization of the two orientations was 47.5 and 52.1 h for the parallel and perpendicular orientations, corresponding to 642 and 753 optimization cycles, respectively. The results of the full optimization are shown in Table 4, and again, it is obtained that the parallel template orientation is the most stable, thus confirming the agreement with the proposed template orientation.[23] In this case the energy difference is 0.07 eV (6.8 kJ/mol), and this suggests that both template orientations, parallel and perpendicular, may be possible.

Regarding the conformation of the template molecule, it was found that in the case of the parallel orientation the three pyrrolidinium rings are puckered toward the same side of the benzene ring whereas in the perpendicular orientation two and one pyrrolidinium rings are puckered to either side of the benzene plane. This resembles the cases of symmetries $C_{3v}$ and $C_s$ in the gas phase, respectively, although in this case the symmetry was not kept due to the interactions with the zeolite walls. As said above, the template has been fully optimized, and therefore the respective conformations have been obtained without imposing any optimization constraint and correspond to the best possible fit of the template to the zeolite topology in each case. The small energy necessary to cross between the template conformations is highly compensated by the optimization of the zeolite−template interactions.

It is not the aim of this work to argue further on whether one or both template orientations, parallel and perpendicular, are actually present in the synthesis of ZSM-18, but rather to analyze the factors that stabilize a given template orientation, and this is done below.

**3.3. Factors Directing the Synthesis of ZSM-18.** When trispyrrolidinium is used as template, the zeolite synthesis—under certain particular conditions of Si/Al ratio, pH, and temperature[41]—gives almost exclusively ZSM-18. This shows an effect of the structure-directing agent which has been justified by the close matching between the shape of the template and the shape of the surrounding micropore. This matching—in a manner similar to that of a hand and a glove—is not obvious from a first view of the structure down the [001] direction, but as was said above the free space available

(41) Ciric, J. U.S. Patent 3,950,496, 1976.

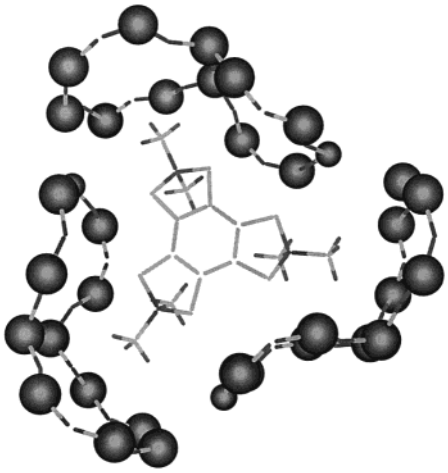

**Figure 3.** Tailored view showing only the template and the immediate neighborhood of the ZSM-18 structure, which corresponds to the six 7-MRs around the main channel of the zeolite. Hydrogen atoms bonded to the pyrrole rings are not shown for clarity.

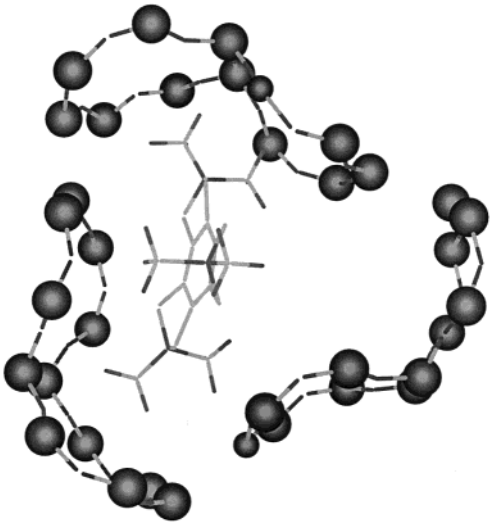

**Figure 4.** Tailored view of showing only the template and the immediate neighborhood of the ZSM-18 structure, which corresponds to the six 7-MRs around the main channel of the zeolite. Hydrogen atoms bonded to the pyrrole rings are not shown for clarity.

in the structure depends on the location of the template down the *z*-axis, the void space being larger at certain heigths in the *z*-axis. This larger room availability has been highlighted in Figure 3 (corresponding to the parallel orientation) and Figure 4 (perpendicular orientation). The careful visualization of these two conformations allows a better understanding of why each conformation looks reasonable, and both may orientate the synthesis to the formation of ZSM-18. The parallel orientation is somewhat more obvious or intuitive. The corresponding two figures (Figures 1 and 3) show a clear and symmetric matching between the template and the large 12-MR channel. Also it is seen (Figure 3) that three out of six methyl groups of the template are directed perfectly into the 7-MRs. Figure 3 shows the six 7-MRs that intersect the 12-MR channel and the three methyl groups that point to the corresponding 7-MRs. On the other hand, the matching between the ZSM-18 void space and the template in its perpendicular orientation (Figures 2 and 4) may be less intuitive in

the sense that (see Figure 2) the template does not fill the 12-MR channel. This *first sight* appreciation would lead to consideration of the perpendicular orientation as not favorable to direct the synthesis toward the ZSM-18 structure, but a more careful look (see Figure 4) unveils a different picture. It can now be seen that it is not the matching between the template and the big channel (12-MRs) that stabilizes the structure in this case but rather the matching between the template and the 7-MRs intersecting the large channel. In this case (Figure 4) five methyl groups of the template are pointing into five corresponding 7-MRs, and this is what causes the necessary matching for the structure-directing ability to appear. The stabilization of both template orientations has therefore been not only justified within the necessary argument of energy minima but also rationalized in terms of matching between the template and zeolite structure.

The ZSM-18 framework contains one 12-MR channel per unit cell, and the matching between the ZSM-18 topology and the template methyl groups precludes the possibility of allowing more than one template molecule per unit cell to fill the zeolite void space. This can be rationalized as follows. In the case of the parallel orientation there is only one "larger room area" in the 12-MR channel per unit cell in which the template can accommodate its methyl groups pointing into the 7-MRs. In the case of the perpendicular orientation, further calculations—not detailed for the sake of brevity—indicated that two template molecules cannot be placed side by side in the channel due to the large repulsive interactions due to the close proximity of the two molecules, and this result seems quite intuitive from inspection of Figure 4 where no room appears available for a second template molecule. Therefore, it seems that a concentration of one template molecule per unit cell is about the optimum for the synthesis of ZSM-18.

**3.4. Does the Template Orientation Influence the Al Distribution in ZSM-18?** As said above the *initial Al distribution* was obtained by minimizing the Al−N distance. In this way, each of the three Al atoms present in the zeolite framework was located in the position closest to the corresponding N atom of the template. This was done because the negative charge brought by Al is expected to locate close to the concentration of positive charge in the methyl groups of the template. Instead of defining a more complicated set of distances between the Al atom and the center of mass of the methyl groups, the closeby N atom (bonded to two methyl groups) was selected instead for the sake of simplicity. For each template orientation an analysis of all the possible T−N (T = Si, Al) distances was performed, and an excerpt of the results is summarized in Table 5. It can be seen that for the parallel orientation the closest T−N distances are 4.26, 4.26, and 4.27 Å, which correspond precisely to the T sites in which the Al has been introduced. Analogously, for the perpendicular orientation the smallest T−N distances are 4.01, 4.20, and 4.68 Å, and they correspond to the places where the three Al atoms have been introduced. A further analysis reveals that the Al atoms have been substituted in positions Al4, Al4, and Al4 (in the parallel orientation case) and in Al2, Al4, and Al3 (in the perpendicular orientation case). Once the initial Al distributions have been justified, a question arises about whether other possible Al distributions may further stabilize any of the template orientations considered, which could change the conclusions stated above on the parallel configuration being the preferred template orientation. To address this point, other Al distributions must be tested. In doing this, and despite the limitations of the subsequent approach, we opted for carrying out "partial" minimizations, in this case by not only keeping the framework atoms fixed to the crystallographic positions but also keeping the template orientation in the conformations previously optimized. This was done because we are only interested in exploring how the Al distributions stabilize the already found template orientations. A series of 100 *random Al distributions* were considered. These Al distributions were generated randomly by a simple algorithm that yields three nonrepeated whole numbers between 1 and 272, which is the number of T atoms in the framework. Al distributions violating the Lowenstein rule[42] were discarded, and the first 100 valid distributions were optimized. This process was performed separately on the parallel and perpendicular orientations, and the corresponding energies are shown in Figure 5. An energy span of about 14 eV was found in both cases (parallel and perpendicular orientations), and these energy differences arise in terms of the resulting electrostatic interaction in each particular case. It can be seen that none of the Al distributions generated result in a lower energy than the initial Al distribution, whose energies, for the parallel and perpendicular cases, range below −34475 eV (see Table 4), whereas all the energies in these random Al distributions lie above −34470 eV (Figure 5). Therefore, it follows that our initial configurations were chosen successfully and they are expected to correspond closely to the experimental Al distribution. Furthermore, the initial Al distributions were chosen on an electrostatic basis trying to maximize the electrostatic attraction between the Al atoms and the positive charge on the

**Table 5. N−T Distances (Å) below 5 Å in the MEI−Template System**

| label | N4 number | T number | distance (Å) |
|---|---|---|---|
| Parallel Orientation (Figure 1) | | | |
| N4−Si2 | 824 | 56 | 4.96 |
| N4−Si2 | 824 | 128 | 4.97 |
| N4−Al4 | 824 | 262 | 4.27 |
| N4−Si1 | 827 | 2 | 4.99 |
| N4−Si2 | 827 | 42 | 4.89 |
| N4−Al4 | 827 | 250 | 4.26 |
| N4−Si1 | 830 | 4 | 5.00 |
| N4−Si2 | 830 | 36 | 4.89 |
| N4−Al4 | 830 | 272 | 4.26 |
| Perpendicular Orientation (Figure 2) | | | |
| N4−Si1 | 824 | 28 | 4.88 |
| N4−Si2 | 824 | 71 | 4.94 |
| N4−Si2 | 824 | 108 | 4.71 |
| N4−Si3 | 824 | 176 | 4.91 |
| N4−Al4 | 824 | 272 | 4.20 |
| N4−Si2 | 827 | 71 | 4.97 |
| N4−Al3 | 827 | 211 | 4.68 |
| N4−Si1 | 830 | 26 | 4.78 |
| N4−Si2 | 830 | 73 | 4.87 |
| N4−Al2 | 830 | 114 | 4.01 |
| N4−Si3 | 830 | 217 | 4.69 |
| N4−Si4 | 830 | 250 | 4.88 |

(42) Lowenstein, W. *Am. Mineral.* **1954**, *39*, 92.

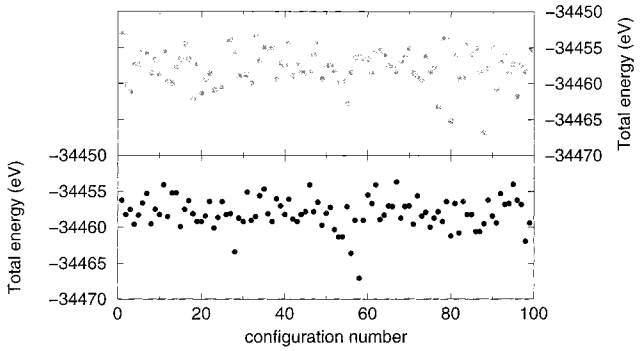


**Figure 5.** Energy (eV) of the zeolite ($Si_{269}Al_3O_{544}$) + template system with 100 different Al distributions generated randomly. Top: parallel orientation of the template. Bottom: perpendicular orientation of the template.

template. The success of this criterion indicates that the Al distributions are shaped by the template orientation so as to minimize the electrostatic total energy. Although obviously other energy terms may come into effect, we believe the electrostatic factor is of major importance in this case. Other computational studies on microporous materials also indicate the importance of electrostatic factors in explaining some of their physicochemical properties.[43,44] It also follows from our results that the Al distribution in ZSM-18 is not decided by the stability of the framework upon Al introduction, which points to a destabilization of the Al4 position (as from Table 3), but rather the Al distribution is governed by the template orientation in the void space of the zeolite framework, a result also observed in recent studies on ZSM-12.[20] In this sense the electrostatic interaction between the Al atoms and the charged template overcomes the factor due to energy differences of Al insertion into the framework. Even more interesting is to draw the conclusion that if, as suggested by the calculations, the parallel template orientation is the most stable and therefore the one that should be expected, the Al atoms will tend to be located in the Al4 positions (this means in the 3-MRs), which is precisely what is hinted by the XRD analysis in which a slightly larger T−O distance is found for the T4−O case (see the T−O distances in Table 2), this meaning that Al tends to locate in the 3-MRs. This corresponds to what is suggested by the authors of the XRD study of ZSM-18.[23] All of these conclusions show that computer simulations are of help in elucidating how the template considered orientates the synthesis toward ZSM-18, and it opens the possibility of using this methodology in other similar cases in the field of zeolite synthesis.

**Acknowledgment.** We thank the Generalitat Valenciana (Project GV01-492) for financial support and $C^4$ (Centre de Computacio i Comunicacions de Catalunya) for the use of their computer facilities. The High Performance Computational Chemistry Group from Pacific Northwest National Laboratory (Richland, WA) is acknowledged for making available NWChem version 4.0, a computational chemistry package for parallel computers.

CM0110526

(43) Sastre, G.; Lewis, D. W.; Corma, A. *Phys. Chem. Chem. Phys.* **2000**, *2*, 177.
(44) Sierka, M.; Eichler, U.; Datka, J.; Sauer, J. *J. Phys. Chem. B* **1998**, *102*, 6397.